Inorg. Chem. **2003**, *42*, 3187–3193

Synthesis and Properties of Rhodium(III) Porphyrin Cyclic Tetramer and Cofacial Dimer

Keiko Fukushima,[†] Kenji Funatsu,[†] Akio Ichimura,[‡] Yoichi Sasaki,[†] Masamitsu Suzuki,[†] Tetsuaki Fujihara,[†] Kiyoshi Tsuge,[†] and Taira Imamura*,[†]

Division of Chemistry, Graduate School of Science, Hokkaido University, Sapporo 060-0810, Japan, and Department of Chemistry, Faculty of Science, Osaka City University, Osaka 558-0022, Japan

Received November 4, 2002

Rhodium(III) porphyrin complexes, $[Rh(4\text{-}PyT_3P)Cl]_4$ (**1**) and $[Rh(2\text{-}PytB_3P)Cl]_2$ (**2**) (4-PyT_3P = 5-(4-pyridyl)-10,15,20-tritolylporphyrinato dianion, 2-$PytB_3P$ = 5-(2-pyridyl)-10,15,20-tri(4-*tert*-butyl)phenylporphyrinato dianion), were self-assembled and characterized by ^{1}H nuclear magnetic resonance spectroscopy, infrared spectroscopy, and electron spray ionization–mass spectroscopy methods. The spectroscopic results certified that the rhodium porphyrin complexes **1** and **2** have a cyclic tetrameric structure and a cofacial dimeric structure, respectively. The X-ray structure analysis of **1** confirmed the cyclic structure of the complex. The Soret bands of both oligomers were significantly broadened by excitonic interactions between the porphyrin units, compared to those observed for a corresponding analogue of Rh(TTP)(Py)Cl (TTP = 5,10,15,20-tetratolylporphyrinato dianion, Py = pyridine). Stepwise oxidation of the porphyrin rings in the oligomers was observed by cyclic voltammetry. The oligomers **1** and **2** are very stable in solution, and they slowly undergo reactions with pyridine to give corresponding monomer complexes only at high temperatures (∼80 °C).

Introduction

Porphyrin assemblies using axial ligand coordination are useful in the construction of functional systems such as molecular electronic devices, redox-active materials, and light-harvesting structures.[1−3] To build up sterically controlled unique metalloporphyrin oligomer systems for these purposes, versatile central metal ions and substituents of porphyrin rings have been investigated.[4,5] We have adopted less-substitutable and redox-active metal ions, such as ruthenium(II), as the central metal ion and coordinative porphyrins with pyridyl groups as building blocks.[6] In a variety of ruthenium(II) pyridylporphyrin oligomers thus prepared, cyclic ruthenium porphyrin tetramers[7] and cofacial ruthenium porphyrin dimers,[8,9] both without X-ray crystal structures,[10] showed characteristic electrochemical and spectroscopic properties caused by interactions between constituent porphyrin units. Rhodium(III) porphyrins are promising candidates as another powerful building block that gives more-stable oligomers with stronger intramolecular interac-

* Author to whom correspondence should be addressed. E-mail: timamura@sci.hokudai.ac.jp.
[†] Hokkaido University.
[‡] Osaka City University.

(1) Chambron, J.-C.; Heitz, V.; Sauvage, J.-P. In *The Porphyrin Handbook*; Kadish, K. M., Smith, K. M., Guilard, R., Eds.; Academic Press: New York, 2000; Vol. 6, Chapter 40, pp 1−42.
(2) Balzani, V.; Scandola, F. In *Comprehensive Supramolecular Chemistry*; Atwood, J., MacNicol, D., Davies, E., Vögtle, F., Lehn, J.-M., Eds.; Pergamon Press: Oxford, U.K., 1996; Vol. 10, Chapter 23, pp 687−746.
(3) Wojaczynski, J.; Latos-Grazynski, L. *Coord. Chem. Rev.* **2000**, *204*, 113−171.
(4) Chou, J.-H.; Kosal, M. E.; Nalwa, H. S.; Rakow, N. A.; Suslick, K. S. In *The Porphyrin Handbook*; Kadish, K. M., Smith, K. M., Guilard, R., Eds.; Academic Press: New York, 2000; Vol. 6, Chapter 41, pp 43−131.
(5) Sanders, J. K. M. In *The Porphyrin Handbook*; Kadish, K. M., Smith, K. M., Guilard R., Eds.; Academic Press: New York, 2000; Vol. 3, Chapter 22, pp 347−368.
(6) Imamura, T.; Fukushima, K. *Coord. Chem. Rev.* **2000**, *198*, 133−156.
(7) Funatsu, K.; Imamura, T.; Ichimura, A.; Sasaki, Y. *Inorg. Chem.* **1998**, *37*, 1798−1804.
(8) Funatsu, K.; Imamura, T.; Ichimura, A.; Sasaki, Y. *Inorg. Chem.* **1998**, *37*, 4986−4995.
(9) Imamura, T.; Funatsu, K.; Ye, S.; Morioka, Y.; Uosaki, K.; Sasaki, Y. *J. Am. Chem. Soc.* **2000**, *122*, 9032−9033.
(10) The formation of a cyclic zinc porphyrin tetramer from 5-(4-pyridyl)-10,15,20-triphenylporphyrinato zinc(II) in solution was also clarified by variable temperature ^{1}H NMR measurements.[7] Very recently, in the preparation of the present paper, the structure of the cyclic tetramer was confirmed for 5-(4-pyridyl)-15-(3,5-di-*tert*-butylphenyl)porphyrinato zinc(II) by X-ray crystal analysis (Tsuda, A.; Nakamura, T.; Sakamoto, S.; Yamaguchi, K.; Osuka, A. *Angew. Chem., Int. Ed.* **2002**, *41*, 2817−2821).

10.1021/ic020652j CCC: $25.00
Published on Web 04/15/2003

Scheme 1

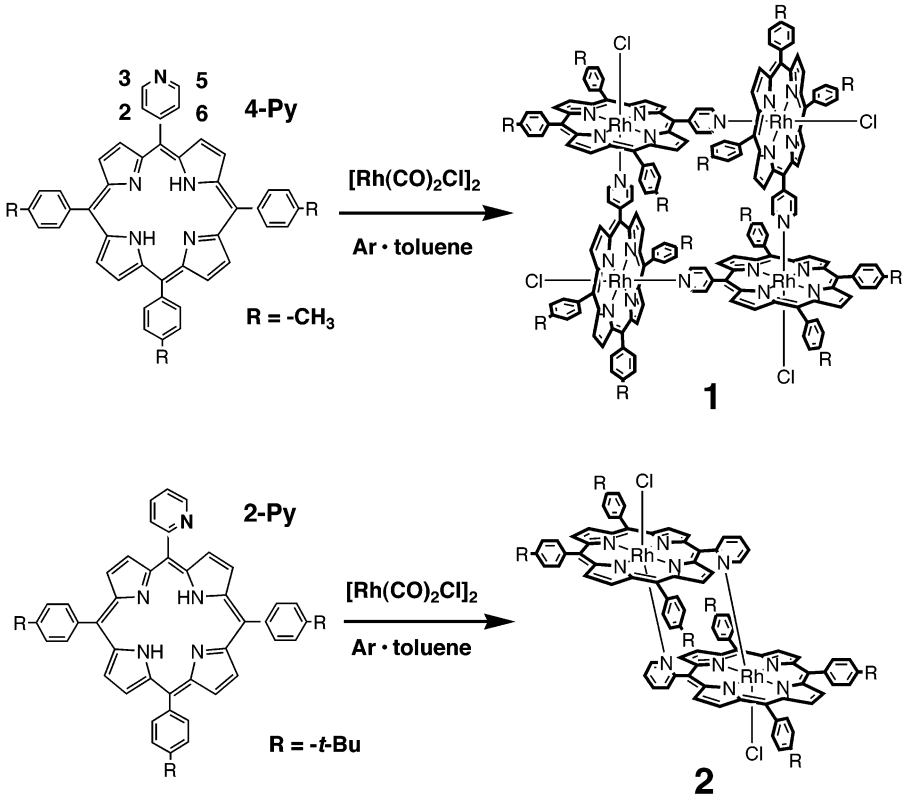

tions, because of their less-substitutable character and the small ionic radius of the Rh(III) ion. Rhodium(III) porphyrins have been practically utilized as versatile building blocks to assemble structurally unique oligomers such as heterometallic porphyrin arrays[11] and a cofacial dimer[12] with two pyridyl groups at trans−meso positions of the constituent porphyrin unit.

Herein, a new cyclic rhodium(III) pyridylporphyrin tetramer and a cofacial dimer are reported (Scheme 1). The structure of the cyclic tetramer was successfully determined by X-ray crystallography. The rhodium(III) porphyrin oligomers showed strong intramolecular interactions in UV−vis spectra and electrochemical data.

Experimental Section

Instrumentation. UV−vis spectra were recorded on Hitachi model U-3410 or model U-3000 spectrophotometers. ^{1}H NMR spectra were recorded on a JEOL model EX270 spectrometer. Cyclic voltammograms (CVs) were recorded with a BAS model CV-50W voltammetry analyzer at a scan rate of 100 mV s^{-1} at 20 °C. The working and counter electrodes for the cyclic voltammetry measurements were a platinum disk (inside diameter of 1.6 mm) and a platinum wire, respectively. The sample solutions in 0.1 M TBA(PF_6)−CH_2Cl_2 were deoxygenated by a stream of argon.[13] The reference electrode was Ag/AgCl. Redox potentials obtained were corrected by the potential of a ferrocenium/ferrocene couple (0.352 V).

X-ray Crystallography. The crystals of [Rh(4-PyT_3P)Cl]$_4$ (**1**) were obtained as $CHCl_3$ and C_6H_{14} solvates, via the diffusion of pentane into the chloroform solution. Structure data were collected on a Rigaku model AFC-8S diffractometer with a Mercury CCD area detector using graphite-monochromated Mo Kα radiation (λ = 0.71073 Å) at 120 K and processed using the Crystal Clear software program.[14] Final cell parameters were obtained from a least-squares analysis of reflections with $I > 10\sigma(I)$. The crystal structure was solved by direct methods and expanded using Fourier and difference Fourier techniques. Atomic coordinates and anisotropic thermal parameters of the non-hydrogen atoms were refined by full-matrix least-squares calculations. The hydrogen atoms were placed at calculated positions. All calculations were performed using the teXsan crystallographic software package.[15]

Materials. Free-base porphyrins containing meso-pyridyl groups—H_2(2-Py)T_3P, H_2(2-Py)tB_3P, and H_2(4-Py)T_3P—were synthesized and characterized by ^{1}H NMR measurements.[8] Rhodium porphyrin monomer, Rh(TTP)(Py)Cl, was synthesized by the reaction of [$Rh^I(CO)_2Cl]_2$ and H_2TTP, with reference to the literature method,[16] and characterized by spectral methods.

(11) Redman, J. E.; Feeder, N.; Teat, S. J.; Sanders, J. K. M. *Inorg. Chem.* **2001**, *40*, 2486−2499.
(12) (a) Aoyama, Y.; Kamohara, T.; Yamagishi, A.; Toi, H.; Ogoshi, H. *Tetrahedron Lett.* **1987**, *28*, 2143−2146. (b) Aoyama, Y.; Yamagishi, A.; Tanaka, Y.; Toi, H.; Ogoshi, H. *J. Am. Chem. Soc.* **1987**, *109*, 4735−4737.

(13) Abbreviations: H_2TTP = 5,10,15,20-tetratolylporphyrin; H_2TPP = 5,10,15,20-tetraphenylporphyrin; H_2(4-Py)T_3P = 5-(4-pyridyl)-10,15,-20-tritolylporphyrin; H_2(2-Py)T_3P = 5-(2-pyridyl)-10,15,20-tritolylporphyrin; H_2(4-Py)P_3P = 5-(4-pyridyl)-10,15,20-triphenylporphyrin; H_2(2-Py)T_3P = 5-(2-pyridyl)-10,15,20-tritolylporphyrin; TTP = 5,-10,15,20-tetratolylporphyrinato dianion; TPP = 5,10,15,20-tetraphenylporphyrinato dianion; OEP = 2,3,7,8,12,13,17,18-octaethylporphyrinato dianion; 4-PyT_3P = 5-(4-pyridyl)-10,15,20-tritolylporphyrinato dianion; 2-PytB_3P = 5-(2-pyridyl)-10,15,20-tri(4-*tert*-butyl)phenylporphyrinato dianion; Py = pyridine; TBA(PF_6) = *n*-tetrabutylammonium hexafluorophosphate.

(14) Data Processing System Software; Rigaku Co.: Tokyo, 1999.
(15) Single-Crystal Structure Analysis Software, Version 1.6; Molecular Structure Co.: The Woodlands, TX, 1993.
(16) Grass, V.; Lexa, D.; Momenteau, M.; Saveant, J.-M. *J. Am. Chem. Soc.* **1997**, *119*, 3536−3542.

Anal. Calcd for $C_{53}H_{41}N_5ClRh$ (Rh(TTP)(Py)Cl): C, 71.83; H, 4.66; N, 7.90; Cl, 4.00. Found: C, 71.59; H, 5.04; N, 8.03; Cl, 3.87. ^{1}H NMR ($CDCl_3$, 270 MHz): H_{CH3} 2.69 (s, 12H), H_o 8.17, 8.20 (dd, 8H), H_m 7.49−7.56 (m, 8H), H_β 8.88 (s, 8H), $H_{2,6-Py}$ 0.96 (d, 2H), $H_{3,5-Py}$ 5.03 (t, 2H), H_{4-Py} 6.02 (t, 1H) ppm. UV−vis (CH_2Cl_2), λ_{max}/nm (ϵ/10^3 M^{-1} cm^{-1}): 427 (276), 536.5 (24.1), 571 (7.84).

[Rh(4-PyT$_3$P)Cl]$_4$ (1). The tetramer **1** was prepared with reference to the methods for Rh(TTP)(Py)Cl [16] and [Ru(4-PyT$_3$P)-(CO)]$_4$.[7] [Rh^I(CO)$_2$Cl]$_2$ (100 mg, 0.26 mmol) and H$_2$(4-Py)T$_3$P (100 mg, 0.15 mmol) were dissolved in 100 mL of toluene under an argon atmosphere in a glovebox. The solution was removed from the glovebox and refluxed for 5 h under an argon atmosphere, filtered through a sintered glass to remove the remaining rhodium complex, and evaporated to dryness. The resulting solid material was again dissolved in dichloromethane. The solution was warmed, mixed with a large excess of 2,3-dichloro-5,6-dicyano-*p*-benzoquinone (DDQ), and chromatographed on a silica gel column using 0.4% methanol−dichloromethane as an eluent. The first eluted red band was collected and evaporated to dryness. The solid product was recrystallized from dichloromethane−pentane and dried at 100 °C in vacuo for 4 h (yield: 41%, 48 mg).

Anal. Calcd for $C_{184}H_{132}N_{20}Cl_4Rh_4$: C, 69.57; H, 4.19; N, 8.82; Cl, 4.46. Found: C, 69.36; H, 4.69; N, 8.20; Cl, 4.19. UV−vis (CH_2Cl_2), λ_{max}/nm (ϵ/10^3 M^{-1} cm^{-1}): 429 (686), 537 (76.7), 576 (23.4). ^{1}H NMR ($CDCl_3$, 270 MHz): H_{CH3} 2.64 (s, 12H), 2.74 (s, 24H), H_o 8.01−8.16 (m, 24H), H_m 7.49−7.77 (m, 24H), H_β 7.00 (d, 8H), 8.52 (d, 8H), 8.73 (d, 8H), 8.95 (d, 8H), $H_{3,5-Py}$ 0.32 (d, 4H), 0.89 (d, 4H), $H_{2,6-Py}$ 5.56 (dd, 4H), 5.96 (dd, 4H) ppm. Electron spray ionization−mass spectroscopy (ESI−MS): 1588.1 (m/Z^+) for [Rh(4-PyT$_3$P)Cl]$_4^{2+}$, 3177.8 (m/Z^+) for [Rh(4-PyT$_3$P)-Cl]$_4^+$.

[Rh(2-PytB$_3$P)Cl]$_2$ (2). [Rh^I(CO)$_2$Cl]$_2$ (100 mg, 0.26 mmol) and H$_2$(2-Py)tB$_3$P (80 mg, 0.1 mmol) were dissolved in 80 mL of toluene in a glovebox under an argon atmosphere. The solution was removed from the glovebox, refluxed for 3 h under an argon atmosphere, passed through a sintered glass, and chromatographed on a silica gel column. Using dichloromethane as an eluent, a pale pink colored band was eluted first and followed by the elution of a red band. The red band was collected and evaporated to dryness. The solid material obtained was dried for 4 h in vacuo (yield: 48%, 45 mg).

Anal. Calcd for $C_{110}H_{102}N_{10}Cl_2Rh_2$: C, 71.77; H, 5.59; N, 7.61; Cl, 3.85. Found: C, 71.03; H, 5.77; N, 7.71; Cl, 3.79. UV−vis (CH_2Cl_2), λ_{max}/nm (ϵ/10^3 M^{-1} cm^{-1}): 421 (232), 547 (45.4), 586 (8.98). ^{1}H NMR (CD_2Cl_2, 270 MHz): H_{t-Bu} 1.71 (s, 18H), 1.73 (s, 36H), $H_{o,m}$ 7.81−8.13 (m, 24H), H_β 5.48 (d, 4H), 8.49 (d, 4H), 9.07 (d, 4H), 9.13 (d, 4H), H_{3-Py} 1.43 (d, 2H), $H_{4,5-Py}$ 5.66 (m, 4H), H_{6-Py} 6.33 (d, 2H) ppm. ESI−MS: 1841.01 (m/Z^+) for [Rh-(2-PytB$_3$P)Cl]$_2^+$, 1804.06 (m/Z^+) for [Rh$_2$(2-PytB$_3$P)$_2$Cl]$^+$.

The treatment of [Rh^I(CO)$_2$Cl]$_2$ with H$_2$(2-Py)T$_3$P gave another dimer complex, [Rh(2-PyT$_3$P)Cl]$_2$, which has a broad Soret band at 420.5 nm and Q-bands at 547.5 and 586.0 nm in dichloromethane. By the addition of pyridine to the solution, the UV−vis spectrum slowly changed to give a spectrum of the corresponding monomer. However, this complex could not be characterized in detail, because of its low solubility in organic solvents, which prevented measurement of the ^{1}H NMR spectrum.

Results and Discussion

Elemental analyses of **1** and **2** were consistent with their respective compositions, as detailed in the Experimental Section. The tetramer **1** showed an ESI−MS peak at 1588.1 (m/Z^+) with 0.5 mass unit, which corresponds to the dication of the tetramer ([Rh(4-PyT$_3$P)Cl]$_4^{2+}$), in addition to the peak of [Rh(4-PyT$_3$P)Cl]$_4^+$ at 3177.8 (m/Z^+) (Figure 1). Although the ESI−MS spectrum with 0.5 mass unit somewhat overlapped the spectrum with 1.0 mass unit of dimer fragments ([Rh(4-PyT$_3$P)Cl]$_2^+$), the spectral feature with 0.5 mass unit indicated the formation of the tetramer. The cofacial dimer **2** showed a parent peak of [Rh(2-PytB$_3$P)-Cl]$_2^+$ at 1841.01 (m/Z^+). ^{1}H NMR spectra of **1** and **2** confirmed the cyclic tetramer structure and the cofacial dimer structure, respectively, and showed the high symmetry of these frameworks in solution. The sharpness of the NMR signals does not contradict diamagnetism of the oligomers; that is, the valence of the Rh ion is 3+.

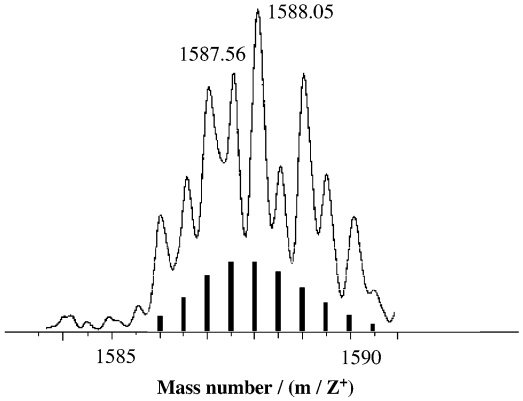

Figure 1. ESI−MAS spectrum of [Rh(4-PyT$_3$P)Cl]$_4$ (**1**) with 0.5 mass unit intervals. The bar graph shows a calculated spectrum of the dication of the tetramer, ([Rh(4-PyT$_3$P)Cl]$_4^{2+}$).

Table 1. Crystallographic Data for **1**·10CHCl$_3$·C$_5$H$_{12}$·2C$_6$H$_{14}$

empirical formula	$C_{211}H_{182}Cl_{34}N_{20}Rh_4$
temp/K	123
cryst syst	triclinic
space group	$P\bar{1}$ (No. 2)
a/Å	15.972(1)
b/Å	17.631(2)
c/Å	19.856(2)
α/deg	86.924(3)
β/deg	86.302(1)
γ/deg	81.108(1)
V/Å^3	5507.2(8)
Z	1
d_{calcd}/g cm^{-3}	1.391
no. of unique reflns	21 837
no. of observed reflns	14 524
R1, wR2[a]	0.102, 0.234

[a] $R1 = \sum||F_o| - |F_c||/\sum|F_o|$, $wR2 = \{\sum[w(F_o^2 - F_c^2)^2]/\sum[w(F_o^2)^2]\}^{1/2}$, $w = \{\sigma^2(F_o^2) + [0.05\ (\max(F_o^2, 0) + 2F_c^2)/3]^2\}^{-1}$.

Cyclic Tetramer 1. The structure of tetramer **1** was determined by X-ray structure analysis. The crystallographic data of [Rh(4-PyT$_3$P)Cl]$_4$ and selected bond lengths and angles are listed in Tables 1 and 2. The molecular structure of the tetramer **1** has a crystallographically imposed inversion center, and two porphyrin units, labeled Rh1por and Rh2por, are independent. One unit cell contains ten chloroform, two hexane, and one pentane molecules as crystal solvents, other than one tetramer molecule. The structure analysis revealed that each pyridyl group of a rhodium porphyrin unit is coordinated to the Rh atom of an adjacent porphyrin unit to

Table 2. Selected Atomic Distances (Å) and Angles (deg) for Complex **1**[a]

Rh1−N1	2.034(7)	Rh2−N5	2.081(7)
Rh1−N2	2.029(7)	Rh2−N6	2.017(6)
Rh1−N3	2.030(7)	Rh2−N7	2.032(7)
Rh1−N4	2.024(7)	Rh2−N8	2.021(6)
Rh1−N10′	2.058(7)	Rh2−N9	2.022(7)
Rh1−Cl1	2.315(2)	Rh2−C12	2.324(2)
Rh1···Rh2	9.684(1)		
Rh1···Rh2′	9.764(1)		
N1−Rh1−N2	90.3(3)	N6−Rh2−N7	90.1(3)
N2−Rh1−N3	89.5(3)	N7−Rh2−N8	89.9(3)
N3−Rh1−N4	90.4(3)	N8−Rh2−N9	89.8(3)
N4−Rh1−N1	89.8(3)	N9−Rh2−N6	90.2(3)
N1−Rh1−N3	179.7(3)	N6−Rh2−N8	178.9(3)
N2−Rh1−N4	179.8(3)	N7−Rh2−N9	179.2(3)
Cl1−Rh1−N10′	179.8(2)	Cl2−Rh2−N5	177.7(2)
N1−Rh1−N10′	89.3(3)	N5−Rh2−N6	92.2(3)
N2−Rh1−N10′	89.5(3)	N5−Rh2−N7	86.3(3)
N3−Rh1−N10′	90.9(3)	N5−Rh2−N8	88.9(3)
N4−Rh1−N10′	90.4(3)	N5−Rh2−N9	92.9(3)

[a] Symmetry transformation used to generate equivalent atoms: ′ $-x, -y, -z$.

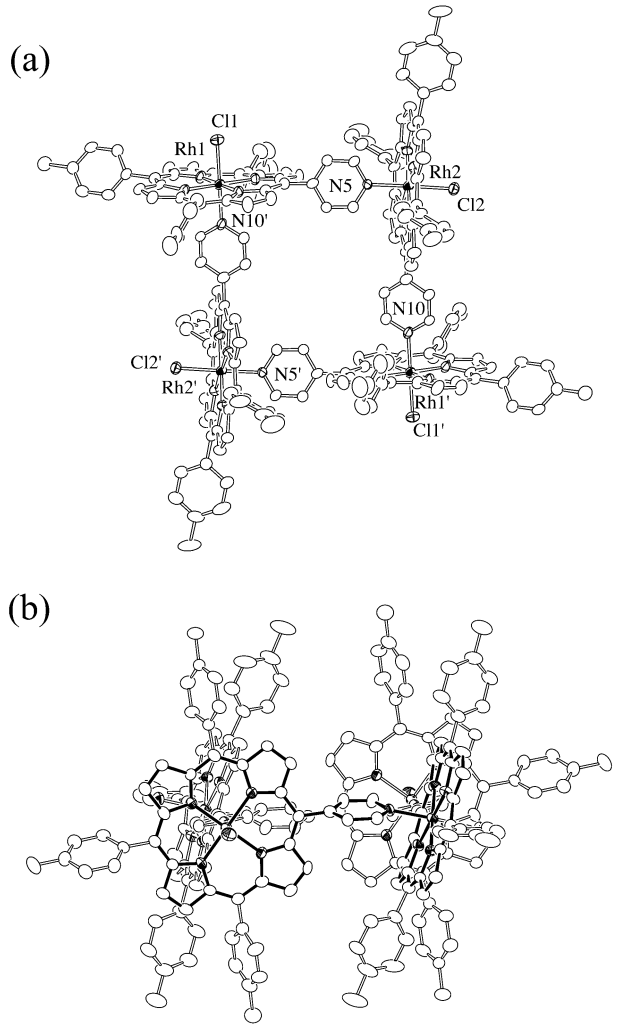

Figure 2. (a) Top view and (b) side view of the molecular structure of $[Rh(4\text{-}PyT_3P)Cl]_4$ **(1)**. Thermal ellipsoids are drawn to illustrate a 50% probability surface.

give the cyclic structure (Figure 2a). Each rhodium porphyrin ring is almost planar. The largest deviation from the 24-atom mean-square plane is 0.22 Å, and the displacement of the Rh ions is 0.01 Å for both Rh1por and Rh2por. The bond distances around the Rh atoms in Rh1por and Rh2por are comparable to those found in other rhodium porphyrins.[11] The dihedral angles of adjacent rhodium porphyrin units were 95.9° and 84.1°, and the distances between cofacially located porphyrins were 9.61 (Rh1por−Rh1′por) and 8.08 Å (Rh2por−Rh2′por). Two pentane and four chloroform molecules are incorporated in the cavity formed by four rhodium porphyrin units (see Figure S1 in the Supporting Information).

The tetramer **1** has C_i symmetry in the crystal. If the tetramer has an idealized symmetric structure—that is, C_{4h} symmetry—the pyridyl groups would be coordinated vertically to the neighboring porphyrin units, as observed in the zinc porphyrin tetramer system,[10] in which the dihedral angles of coordinating pyridyl groups and zinc porphyrin units are 87°−93°. However, in the tetramer **1**, the dihedral angles of coordinating pyridyl groups and rhodium porphyrins were 87.8° and 108.6° for Rh1por and Rh2por, respectively. The latter angle largely deviated by 18.6° from the idealized C_{4h} structure (Figure 2b). By this distortion, the peripheral tolyl groups are located asymmetrically against the virtual C_4 axis and mirror plane.

As shown in Figure 3, the cyclic tetramer molecules stack with eight peripheral tolyl groups to form the channel structure along the *a*-axis. The tetramer chains along this *a*-axis also contact neighboring chains with four tolyl groups sticking out vertically toward the *a*-axis. By this molecular arrangement, not only the channels composed of the intramolecular cavity but also the channels between neighboring tetramer units run along the *a*-axis. The crystal solvents are accommodated in these channels (see Figure S2 in the Supporting Information). In this crystal packing, the distortion of tetramer molecules eliminates the confliction of mutual tolyl groups.

In $CDCl_3$, the ^{1}H NMR signals of the pyridyl and β-pyrrole groups showed very large upfield shifts, which indicates the coordination of rhodium porphyrin units to the axial positions of adjacent rhodium porphyrin units through pyridyl groups to form the cyclic tetramer (see Figure S3 in the Supporting Information). Each rhodium porphyrin unit in the tetramer framework is equivalent in solution. Pyridyl protons in the 3,5- and 2,6-positions gave two sets of upfield-shifted double-doublet peaks distinctly at ∼0.5 and 6 ppm, respectively. The magnitude of the shifts is larger than that of the $[Ru(4\text{-}PyT_3P)(CO)]_4$ system, as discussed in the latter section of "Intramolecular Interactions". One set of the 3,5- and 2,6-protons in a pyridyl group is directed to the outside of the framework, and the other set of protons is directed to the inside of the framework. The integral intensity of each pyridyl proton signal is equivalent to four protons. This assignment was verified by H−H COSY measurements. The β-pyrrole protons gave four signals resulting from their positions. The integral intensity of each β-pyrrole signal corresponds to eight protons. Thus, the ^{1}H NMR results show that the tetramer **1** is stably present in solution.

Cofacial Dimer 2. The dimer complex of $[Rh(2PyT_3P)Cl]_2$ synthesized preliminary was hardly soluble in organic

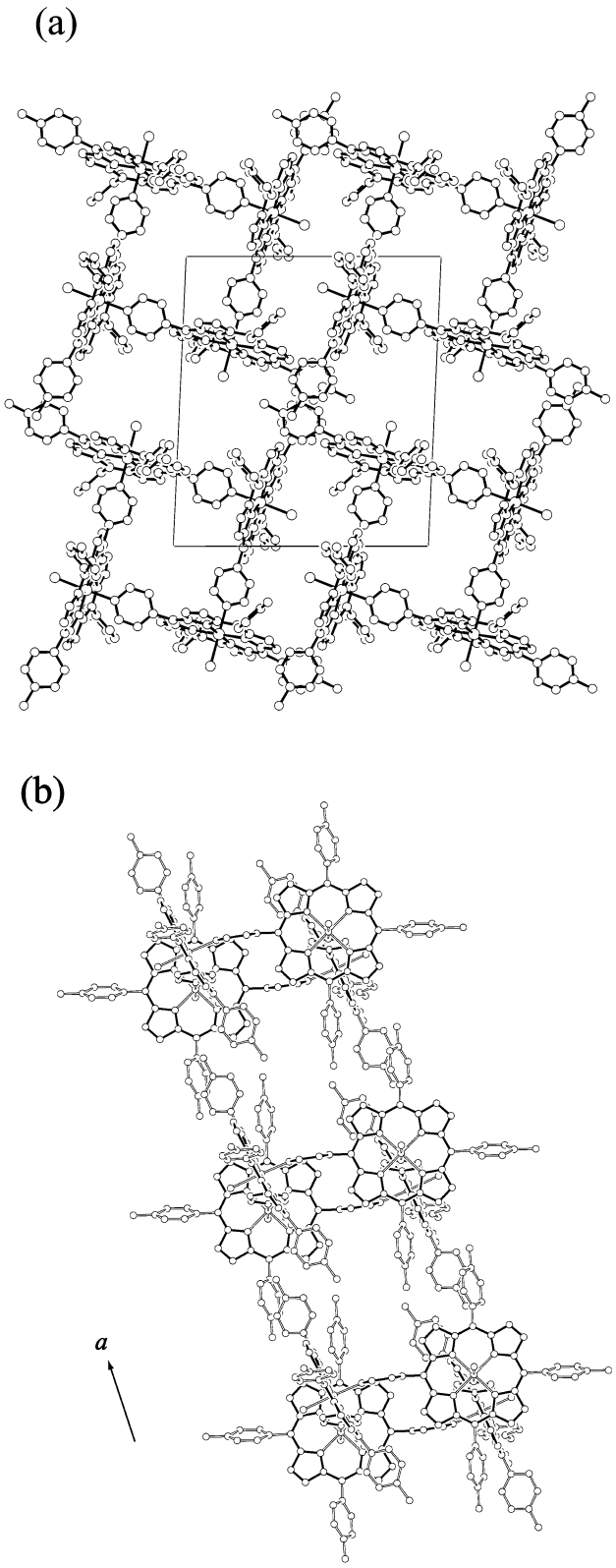

Figure 3. (a) View from *a*-axis and (b) side view of the molecular structure of [Rh(4-PyT$_3$P)Cl]$_4$ **(1)**.

solvents; therefore, the dimer complex **2** of [Rh(2-PytB$_3$P)-Cl]$_2$ with bulky substituents was prepared and characterized. The assignment of the ^{1}H NMR spectrum was achieved by H−H COSY measurements (see Figures S4 and S5 in the Supporting Information). The proton signals of the 2-pyridyl

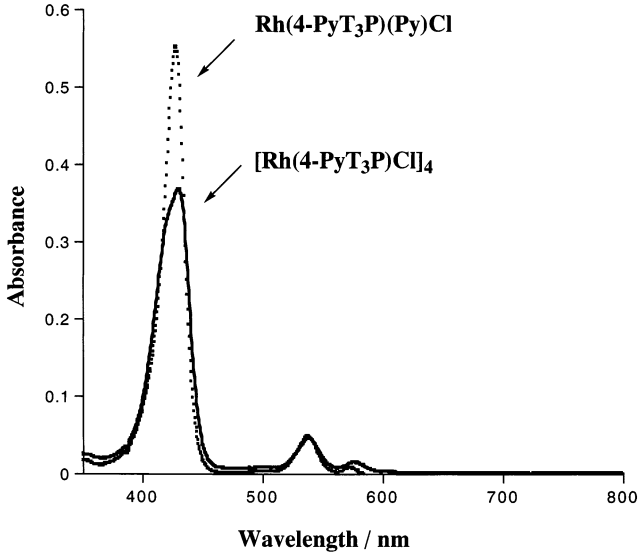

Figure 4. UV−vis spectra of [Rh(4-PyT$_3$P)Cl]$_4$ **(1)** and Rh(4-PyT$_3$P)-(Py)Cl in toluene at 20 °C. Rh(4-PyT$_3$P)(Py)Cl was formed by the addition of a large amount of pyridine (250 equiv per porphyrin unit) to the tetramer solution at 80 °C.

groups shifted from 8−9 ppm for corresponding monomers to 0−6 ppm of high magnetic fields, as observed in cofacial porphyrin dimers such as analogous rhodium,[12a] ruthenium,[8] and zinc complexes.[17,18] The magnitude of the shifts is comparable with the corresponding ruthenium porphyrin dimer system (vide infra). β-Proton signals also shifted to higher magnetic fields in the order of $\beta1 > \beta2 > \beta3 > \beta4$, where β1-protons are the closest to the center of another porphyrin unit.

Stability of Rhodium Porphyrin Oligomers in Solution. The ^{1}H NMR measurements of **1** at various temperatures verified the rotation of the pyridyl groups at ∼100 °C without cleavage of the tetrameric framework. However, the addition of a large amount of pyridine to the solution of the tetramer **1** at high temperatures caused decomposition of the framework to give the monomer. Different from the ruthenium system, in which decomposition of the framework occurred even at room temperature in the presence of 100 equiv of pyridine,[7] the decomposition of the rhodium porphyrin tetramer **1** needs higher concentrations of pyridine and higher temperatures. By the addition of 250 equiv of pyridine per rhodium porphyrin unit to the toluene solution of **1** at 80 °C, the UV−vis spectrum changed to a sharper spectrum in 12 h, as shown in Figure 4. In the progress of the reaction, the peaks (λ_{max} = 429.5, 538.0, 575.5 nm) slightly shifted to shorter wavelengths (λ_{max} = 427.0, 537.5, 573.5 nm) to give the corresponding monomer of Rh(4-PyT$_3$P)(Py)Cl. The half-widths of the peak of **1** at 429.5 nm and of Rh(4-PyT$_3$P)-(Py)Cl at 427.0 nm are 1800 and 1130 cm^{-1}, respectively. The final spectrum of the product, Rh(4-PyT$_3$P)(Py)Cl, is 1.4 times as intense as the Soret band of the initial complex **1**.

The dimer **2** is also robust in solution. When the toluene solution of **2** containing 1000 equiv of pyridine per porphyrin

(17) Kobuke, Y.; Miyaji, H. *J. Am. Chem. Soc.* **1994**, *116*, 4111−4112.
(18) Stibrany, R. T.; Vasudevan, J.; Knapp, S.; Potenza, J. A.; Emge, T.; Schugar, H. J. *J. Am. Chem. Soc.* **1996**, *118*, 3980−3981.

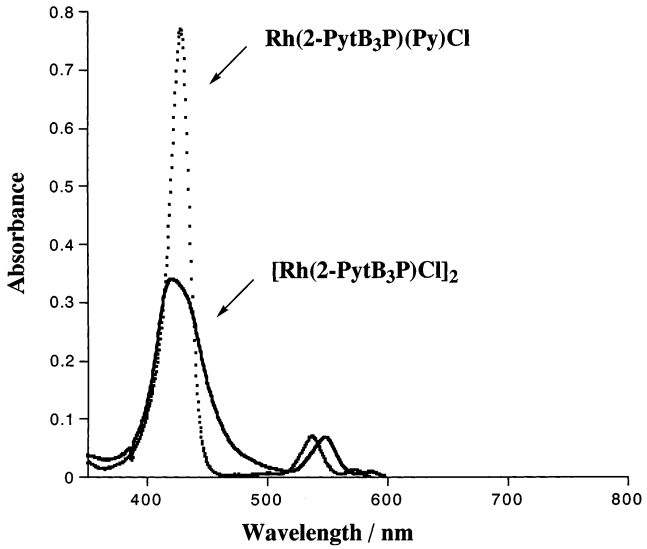

Figure 5. UV−vis spectra of $[Rh(2\text{-}PytB_3P)Cl]_2$ **(2)** and $Rh(4\text{-}PytB_3P)(Py)Cl$ in toluene at 20 °C. $Rh(4\text{-}PytB_3P)(Py)Cl$ was formed by the addition of a large amount of pyridine (1000 equiv per porphyrin unit) to the dimer solution at 80 °C.

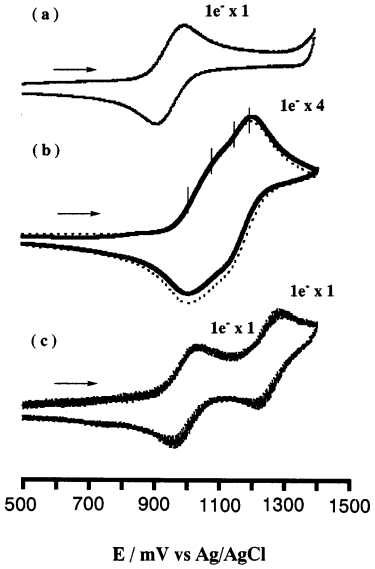

Figure 6. Cyclic voltammograms of rhodium porphyrin complexes in 0.1 M $TBA(PF_6)-CH_2Cl_2$ solution. Plot a shows data for Rh(TTP)(Py)Cl, plot b shows data for $[Rh(4\text{-}PyT_3P)Cl]_4$ **(1)** ((—) experimental data and (···) simulation), and plot c shows data for $[Rh(2\text{-}PytB_3P)Cl]_2$ **(2)**.

unit was left to stand at 80 °C, the broad band at 420.0 nm (half-width of 2480 cm^{-1}) changed to a sharp spectrum of $Rh(2\text{-}PytB_3P)(Py)Cl$ with a peak at 428 nm (half-width of 1075 cm^{-1}) (Figure 5). The final spectrum of the monomer, $Rh(2\text{-}PytB_3P)(Py)Cl$, shows a 2.27-fold increase in intensity, compared to the dimer **2**. It became obvious that the rhodium porphyrin oligomers are very stable to substitution at room temperature. This is a remarkable result because, in ruthenium porphyrin systems, the same reaction proceeds in a few minutes at room temperature.

Intramolecular Interactions. The intramolecular interactions in **1** and **2** were studied by cyclic voltammetry and UV−vis spectral measurements and discussed in comparison to the structural data and the ^1H NMR spectra. The tetramer **1** showed a broad oxidation peak of the porphyrin rings at ∼1100 mV (Figure 6b). The spectral simulation clarified that the oxidation mediates four one-electron steps and proceeds step by step. The first ring oxidation proceeds at 1013 mV (the half-wave potential is denoted as $E^{\circ\prime}$). From the redox data shown in Table 3, it is obvious that there are strong intramolecular interactions between the constituent porphyrin units; that is, the difference in the half-wave potentials between the first ring oxidation and the fourth ring oxidation is ∼173 mV. The value of 173 mV in **1** is significantly larger than that of the ruthenium system (128 mV).[7] The differences of the potentials between the first and second oxidation steps, the second and third oxidation steps, and the third and fourth oxidation steps are 64, 64, and 45 mV, respectively. In the $[Ru(4\text{-}PyT_3P)(CO)]_4$ complex,[7] the first porphyrin ring oxidation occurs at 998 mV ,[19] followed by stepwise oxidation of the remaining porphyrins. The differences of the potentials in the ruthenium system increase as the increment of the oxidation step increases (that is, 18, 49, and 61 mV, respectively).[7] The oxidation number of the central metals

Table 3. Redox Potentials and Potential Differences[a]

complex	first ring oxidation $E^{\circ\prime}$/mV	first ring oxidation ($\Delta E^{\circ\prime}$/mV)	($\Delta E^{\circ\prime}_{total}$/mV)
Rh(TTP)(Py)Cl	955	0	0
$[Rh(4\text{-}PyT_3P)Cl]_4$ **(1)**	1013	64	
	1077	64	173
	1141	45	
	1186		
$[Rh(2\text{-}PytB_3P)Cl]_2$ **(2)**	998		265
	1263		

[a] $E^{\circ\prime}$ denotes the half-wave potential vs Ag/AgCl in 0.1 M $TBA(PF_6)-CH_2Cl_2$. Redox potentials were corrected by the potential of a ferrocenium/ferrocene couple (0.352 V).

must be responsible for the difference in oxidation behavior between the two systems, even for porphyrin ring oxidation, although the electrostatic effects on the porphyrin rings are not formally different between Ru(+2)CO(0)−Por(−2) and Rh(+3)Cl(−1)-Por(−2). Although the value of the half-wave potential (1013 mV at the first oxidation of **1**) is 58 mV larger than that of the corresponding monomer of Rh(TTP)-(Py)Cl without pyridyl groups (955 mV), there is no essential difference in the ease of the first oxidation between the tetramer and the corresponding monomer with a pyridyl group. The replacement of a tolyl group of H_2TTP by a pyridyl group should increase the potential by 45 mV, as suggested by the difference in the reduction potential between H_2TPP and $H_2(4\text{-}Py)P_3P$.[20]

The UV−vis spectral intramolecular interactions of the tetramer **1** are stronger than those of the ruthenium tetramer complex, $[Ru(4\text{-}PyT_3)(CO)]_4$; that is, the formation of the tetrameric structure in the rhodium system **1** has a small molar absorptivity (1.7×10^5 M^{-1} cm^{-1} per porphyrin unit), which corresponds to 62% of Rh(TTP)(Py)Cl (2.8×10^5 M^{-1} cm^{-1}), whereas the ruthenium tetramer has 71% (2.0

(19) This value was corrected by adding 263 mV to the original value of 735 mV vs Ag/Ag^+.

(20) Williams, G. N.; Williams, R. F. X.; Lewis, A.; Hambright, P. *J. Inorg. Nucl. Chem.* **1979**, *41*, 41−44.

$\times 10^5$ M^{-1} cm^{-1}) of the corresponding monomer (2.8×10^5 M^{-1} cm^{-1}). Thus, both electrochemical and UV−vis spectral measurements showed that, in the tetramer systems, the interactions of the rhodium tetramer **1** are stronger than those of the ruthenium tetramer. This result must be mainly ascribed to the shorter interplanar separation, originated from the smaller ionic radius of the Rh(III) ion,[21] of the constituent porphyrin planes in the rhodium(III) tetramer system. Actually, the distance of the (Cl)Rh−N(Pyridyl) bond (2.07 Å on average) in the tetramer **1** is significantly shorter than that of the (CO)Ru−N(Py or Pyridyl) bond in Ru(TPP)(CO)(Py) (2.19 Å)[22] and Ru(OEP)(CO)($H_2$4-PyP_3P) (2.23 Å).[23] This assumption explains well the relatively strong intramolecular interactions in **1** and is consistent with the larger ^{1}H NMR upfield shifts (0.32, 0.89 ppm) of 3,5-pyridyl protons in [Rh(4-PyT_3P)Cl]$_4$, compared with those (0.95, 1.68 ppm)[24] of [Ru(4-PyT_3P)(CO)]$_4$.

On the other hand, in the dimer systems, there is no difference between the rhodium system and the ruthenium system in the magnitude of intramolecular interactions evaluated electrochemically and UV−vis spectrally. The CV of **2** is shown in Figure 6c. The solubility in CH_2Cl_2 is very low; therefore, the concentration of the sample solution was adjusted to 0.25 mM. As expected from the electrochemical results of ruthenium systems,[8] the constituent porphyrin rings of **2** were also oxidized stepwise. One of the two porphyrin units in **2** was first oxidized at 998 mV, followed by the second one-electron oxidation of the other porphyrin unit at 1263 mV. The difference in potential between the first oxidation step and the second oxidation step is 265 mV, which is comparable to 274 mV of [Ru(2-PytB_3P)(CO)]$_2$.[8] The Soret band of **2** is extremely broadened by excitonic interactions between constituent porphyrins; that is, the molar absorptivity per each constituent porphyrin unit is 1.16×10^5 M^{-1} cm^{-1} (half-width of 2490 cm^{-1}), which is 42% of 2.76×10^5 (half-width of 1130 cm^{-1}) for the corresponding monomer. The strong intramolecular interaction spectrally observed (UV−vis) for **2** is again almost the same as for the ruthenium dimer system. The strong geometrical requirements for porphyrin−porphyrin interactions are the result of $\pi-\sigma$ attractions that overcome $\pi-\pi$ repulsions;[25] thus, a favorable interplanar separation could be attained. For zinc porphyrin dimers, it was predicted to be 3.4 Å for the 24-atom porphyrin unit.[25] Actually, the interplanar separation of a cofacial zinc porphyrin dimer was 3.3 Å.[18] This result suggests that the interplanar separations in both the rhodium porphyrin dimer and the ruthenium porphyrin dimer are not so different from each other, which may give rise to almost the same intramolecular interactions in the dimer systems. As expected, the chemical shifts of the pyridyl protons in both the dimer systems are almost the same, that is, H_{3-Py} 1.43 (1.79), $H_{4,5-Py}$ 5.66 (5.74), and H_{6-Py} 6.33 (6.33) ppm for [Rh(2-PytB_3P)Cl]$_2$ (**2**) ([Ru(2-PytB_3P)(CO)]$_2$).[8]

Conclusion

Rhodium(III) porphyrin tetramer and dimer compounds were synthesized and characterized. The structure of the tetramer was determined by X-ray crystallography. UV−vis spectra of these oligomers showed broad Soret bands, as observed in the systems of the corresponding ruthenium porphyrin oligomers. These rhodium porphyrin oligomers underwent reactions at high temperatures with large amounts of pyridine to give corresponding monomer complexes. Sharpening and increasing intensity in the Soret bands, accompanied by the progress of the monomerizations in these oligomers, indicates the presence of excitonic interactions between the porphyrin units. Electrochemical analyses revealed that the ring oxidation processes in these systems proceed stepwise. The potential difference ($\Delta E^{\circ\prime}_{total}$) of the oxidation step in the dimer system was 265 mV. This value is very large, compared to that obtained by the simulation for the system of the cyclic tetramer.

Supporting Information Available: X-ray crystallographic files in CIF format and five figures (Figures S1−S5). This material is available free of charge via the Internet at http://pubs.acs.org.

IC020652J

(21) Shannon, R. D. *Acta Crystallogr.* **1976**, *A32*, 751−767. The ionic radius (0.665 Å) of the Rh(III) ion is smaller than that (0.68 Å) of the Ru(III) ion; therefore, the ionic radius of the Rh(III) ion must be significantly smaller than that of the Ru(II) ion.

(22) Little, R. G.; Ibers, J. A. *J. Am. Chem. Soc.* **1973**, *95*, 8583−8590.

(23) Funatsu, K.; Kimura, A.; Imamura, T.; Ichimura, A.; Sasaki, Y. *Inorg. Chem.* **1997**, *36*, 1625−1635.

(24) The values are the upfield shifts of 2,6-pyridyl protons of [Ru(2-PytB_3P)(CO)]$_2$ in ref 7, where the term "2,6-pyridyl protons" was used instead of "3,5-pyridyl protons".

(25) Hunter, C. A.; Sanders, J. K. M. *J. Am. Chem. Soc.* **1990**, *112*, 5525−5534.